Transcription elongation through lac repressor-mediated DNA loops

Wenxuan Xu[1]*, Yan Yan[1]*†, Irina Artsimovitch[2], Nicolas Sunday[2], David Dunlap[1], Laura Finzi[1]

[1]Physics Department, Emory University, Atlanta, GA, USA

[2] Department of Microbiology, The Ohio State University, Columbus, OH, USA

*Co-first authors

†Current address: Wyss Institute for Biologically Inspired Engineering, Harvard University, Boston, MA, USA

Abstract

During elongation, RNA polymerase (RNAP) must navigate through proteins that decorate genomic DNA. Several of these mediate long-distance interactions via structures, such as loops, that alter DNA topology and create torsional barriers. We used the tethered particle motion (TPM) technique and magnetic tweezers to monitor transcription of DNA templates in the presence of the *lac* repressor (LacI) protein which could bind at two sites, one proximal to, and one distal from, the promoter. The bivalent LacI tetramer binds recognition sites (operators) with up to nanomolar affinity depending on the sequence, and the concentration of LacI was adjusted to promote binding to either one or both operators, so as to produce unlooped or looped DNA. We observed that RNAP pausing before a LacI-securing loop was determined not by the affinity of LacI for the operator, but by the order in which the elongating RNAP encountered these operators. TPM experiments showed that, independent of affinity, LacI bound at the promoter-proximal operator became a stronger roadblock when securing a loop. In contrast, LacI bound to the distal operator was a weaker roadblock in a looped configuration suggesting that RNAP might more easily displace LacI obstacles within a torsion-constrained DNA loop. Since protein junctions can efficiently block the diffusion of DNA supercoiling, these data indicate that the positive supercoiling generated ahead of a transcribing RNAP may facilitate the dissociation of a roadblock. In support of this idea, magnetic tweezers measurements indicated that pauses are shorter when RNAP encounters obstacles on positively supercoiled than on relaxed DNA. Furthermore, at similar winding levels of the DNA template, RNAP pause duration decreased with tension. These findings are significant for our understanding of transcription within the crowded and tensed nucleoid.

Introduction

DNA in the cell is decorated by proteins and adopts a highly compacted structure which includes protein-mediated loops and supercoiling [1-11]. Genome-bound proteins can be roadblocks that hinder elongation by RNA polymerase (RNAP) during transcription[12]. The strength of such roadblocks may be affected by protein-induced topological rearrangements in the DNA, as it happens, for example, when a protein wraps DNA or secures a DNA loop. While transcription

through nucleosomes has been studied [13-15], the RNAP must be able to navigate through many other DNA-bound proteins. Many transcription factors and nucleoid-associated proteins from organisms spanning all kingdoms recognize specific sites (operators) on DNA to shape the genome and regulate transcription. Unlike nucleosomes, these “simple” roadblocks are not subjected to post-translational modifications and remodelling; instead, they respond to environmental cues such as concentration, the presence of multiple operators to which they bind with different affinities, and DNA supercoiling. When bound to multiple operators, they determine architectural DNA modifications such as DNA bending, wrapping and looping [5, 16-23], the role of which has not been addressed in earlier studies on transcription roadblocks *in vivo* and is just beginning to be investigated *in vitro* [24].

In this study, we chose the well characterized *lac* repressor (LacI) protein, from *E. coli*, as a model transcription roadblock inducing topological rearrangements[25]. As a tetramer with two DNA binding domains, LacI can either bind to one specific DNA sequence (operator), or to two operators simultaneously, mediating a loop. There is evidence, from AFM studies, that these two different topologies constitute different types of roadblocks to an elongating RNAP[24]. The strength of the transcription roadblock depends on its affinity for the operator(s) and on cooperativity which increases the effective local concentration of the protein near its operator(s) [26] and loop stability. Using a DNA template containing a weak operator (O2) proximal to and a strong operator (O1) further downstream from the promoter, it was shown that a LacI-mediated loop turns the weak promoter-proximal operator into a roadblock of strength equivalent to that of the strong operator[24]. However, the mechanism by which RNAP transcribes through the entire loop region and the effect of the loop on the promoter-distal operator have not been investigated. Here, we used tether particle motion (TPM) microscopy to monitor transcription through a LacI-mediated loop. Our results confirm that LacI-mediated looping enhances the efficiency of the promoter-proximal roadblock. Surprisingly, we also found that RNAP paused for long times inside the loop region and that the loop weakened the promoter distal roadblock. According to the twin-domain model [27], an elongating RNAP generates negative supercoiling upstream and positive supercoiling downstream. Given that a protein-mediated loop acts as a barrier against diffusion of supercoiling [28], we hypothesized that negative supercoiling behind RNAP inside the loop stabilizes the binding of LacI at the proximal operator [29, 30], whereas the positive supercoiling accumulated ahead of RNAP may destabilize LacI at the distal operator, thereby reducing its strength as a roadblock.

Although it has been shown that transcription-generated positive supercoiling can destabilize nucleosomes [31], it is still not clear how supercoiling affects the binding affinity of other transcription factors and what is the interplay between it and the topologies these factors induce. Thus, we used magnetic tweezers (MTs) to test the effect of supercoiling on LacI binding to DNA and RNAP elongation. Our results demonstrate that RNAP pausing in front of the LacI-O1 obstacle is suppressed when the DNA template is positively supercoiled, supporting the idea that transcription within a LacI-mediated loop stabilizes LacI at the proximal operator and promotes its dissociating from the distal operator. These findings suggest that accumulation of positive supercoiling inside the LacI-mediated loop helps RNAP to exit the loop and may explain how RNAP elongates through specifically bound proteins which mediate long-range interactions.

In summary, this study reveals complex effects of protein-stabilized loops on the kinetics of RNA chain elongation. The LacI-mediated loops lengthen the pause time in front of the promoter-proximal binding site, shorten the pause time in front of the promoter-distal binding site, and increase the frequency of pausing within the loop. We conclude that DNA loops can be potent

transcription roadblocks that can temporarily sequester RNAP, until positive supercoiling build up breaks the loop and enables RNAP escape. The significance of these findings is that *in vivo*, should RNAP become trapped in loops due to long-range interactions, the enzyme has an intrinsic ability to generate sufficient positive supercoiling to free itself from the loop and complete the synthesis of the nascent RNA chain.

Materials and Methods

Preparation of DNA constructs

DNA fragments for TPM experiments (Figure S1A) were constructed using different plasmids depending on the sequence of LacI operators needed. In all the following text and in the figures, O_{prox} indicates the promoter-proximal site, while O_{dist} is the promoter-distal operator. (O_{prox}, O_{dist}) is (O1,O2) in constructs derived from plasmid pWX_12_400 (sequence in SI), while it is (O2,O1) in constructs derived from pZV_21_400 [32], while constructs containing a single O1 operator were derived from pRS_1N_400 or pYY_N1_400. All fragments were amplified by PCR with dNTPs (Fermentas-Thermo Fisher Scientific Inc., Pittsburgh, PA, USA), biotin-labeled, or unlabeled anti-sense primers (Integrated DNA Technologies, Coralville, IA, USA) and Taq DNA Polymerase (New England BioLabs, Ipswich, MA, USA).

DNA tethers used in the MTs measurements were built by ligating with T7 DNA ligase (New England Bio- Labs, Ipswich, MA, USA) a 4098 bp-long main fragment containing the promoter-proximal O_1 operator to a ~150 bp-long multiple biotin-labeled DNA fragment at the promoter-distal end. This “tail” was needed to anchor the main DNA fragment, through multiple attachment sites, to a streptavidin-coated bead, so that torsion could build-up (Figure S1B). The main fragment was a PCR amplicon produced using an equimolar dNTP mix and a primer including ApaI restriction digest site (Table S1). Digestion of the amplified main fragment was then purified for later ligation. The ~150 bp biotin-labeled DNA anchoring tail was generated by ApaI restriction in the middle of a 302 bp-long PCR amplicon produced using dATP, dCTP, dGTP, dTTP (Fermentas-Thermo Fisher Scientific Inc., Pittsburgh, PA, USA) and biotin-11-dUTP (Invitrogen, Life Technologies, Grand Island, NY, USA) in a molar ratio of 1:1:1:0.7:0.3. The ligation product was then purified.

All constructs contained a stall site at the +22 position downstream from the T7A1 promoter where the first “C” is needed following the transcription of a C-less region.

Table S1 summarizes the name of the plasmids, primers and restriction enzymes, as well as the sequence of the primers used.

Preparation of RNAP

Doubly-HA tagged *E. coli* RNA polymerase was used in both TPM and MTs experiments. The *E. coli* RNA polymerase used in TPM experiment was a generous gift by Karen Adelman, Harvard. The *E. coli* RNA polymerase used in MTs experiment was provided by Irina Artsimovitch, OUS, and was purified as described previously [33].

Microchamber preparation

The bottom coverslip of the microchamber (Fisherbrand, Thermo Fisher Scientific, Waltham, MA, USA) supported a parafilm gasket obtained with a laser cutter (Universal Laser Systems, VLS 860, Middletown, CT) with inlet and outlet reservoirs, at the edges of the top coverslip, connected through narrow inlet and outlet channels to the central observation area under the coverslip (Figure S2). The parafilm and coverslips assembly was heated to seal its components together and form the microchamber. The narrow inlet and outlet reduced evaporation of buffer, while the triangular shape of the chamber, confined the reaction in a relatively small volume and provided a gradient of tether densities which helped finding the optimal density.

The entire sample preparation was performed at room temperature (~25 °C) and materials were kept on ice. The beads used in experiments were cleaned as first being washed with phosphate buffered saline (PBS) solution twice, then with basic wash buffer (BWB) (20 mM Tris-Cl (pH 7.4), 50 mM KCl, 1 mM DTT) once and finally resuspended in designed buffer. The chambers were first incubated with BWB resuspended beads for 5 minutes to let some beads stick to the surface and serve as reference during data acquisition and analysis. The chambers were then incubated with 10 μg/ml purified Anti-HA 11 Epitope tag antibody (BioLegend, San Diego, CA, USA) in BWB at room temperature for 1 hour. The surface was then passivated with BWB supplemented with 6 mg/ml α-casein at 4 °C overnight. 60 nM doubly-HA tagged *E. coli* RNA polymerase (Karen Adelman, Harvard, for TPM experiments and Irina Artsimovitch laboratory, OUS, for MTs experiments) were then drawn into the chamber and incubated 30 min at room temperature to let the HA-labeled RNA polymerase bind to the anti-HA coated surface. 10 nM DNA template, 50 µM GpA (initiating dinucleotide, TriLink Bio Technologies, San Diego, CA, USA), and 10 µM ATP/UTP/GTP in transcription buffer (TXB) (20 mM Tris-glutamate (pH 7.4), 10 mM magnesium glutamate, 50 mM potassium-glutamate, 0.2 mg/mL α-casein (Sigma-Aldrich, St. Louis, MO), 1 mM DTT) were introduced into the chamber to produce the stalled elongation complexes (SECs). For TPM experiments, the end of the DNA far from the promoter was then labeled with beads (0.32 μm diameter, streptavidin-coated polystyrene beads (Roche Life Science, Indianapolis, IN, USA)) by flowing TXB resuspended 0.03 mg/mL beads in the microchamber and incubating for 10 min. For MTs experiments, instead, a TXB resuspended 0.02 mg/mL solution of 1.0 μm diameter, streptavidin-coated superparamagnetic beads (Dynabead MyOne Streptavidin T1, Invitrogen, Grand Island, NY)) was incubated for 5 min. Both types of beads were washed in PBS and resuspended in TXB before introducing them into the chamber. The experimental construct for TPM/MTs is schematically illustrated in Figure S1. The extension of the DNA tether was monitored before, to control the original tether length, and after introducing 1 mM NTPs with/without LacI in TXB.

Tether Particle Microscopy (TPM) and TPM data analysis

TPM has been described in detail elsewhere [34]. All TPM experiments were conducted at room temperature. The lamp of the microscope was turned on approx. 1-2 hours before recording the motion of the beads to avoid drift during thermal equilibration. Five immobilized beads were used to calculate the drift, which was then subtracted from the tethered particles' data [34, 35]. The absolute *x, y* positions of each chosen bead were recorded at 50 Hz with a customized Labview (National Instruments, Austin, TX, USA) software. The excursion of each tether was then calculated as $<\rho>_{4s}=<\sqrt{(x-<x>_{4s})^2+(y-<y>_{4s})^2}>_{4s}$. Where $(<x>_{4s},<y>_{4s})$ represents a four-second moving average of the coordinates of the anchor point of the bead. The TPM parameter <ρ> was also determined as a four-second moving average of the raw data.

Changes in the bead excursion reflected any tether length change in the DNA tether[36-38]. The recorded *x, y* data were then analyzed for symmetry and original tether length (before transcription). Beads that exhibited (*x, y*) position distributions with a ratio of the major to minor axes greater than 1.07, were discarded, since they were likely to be tethered by multiple DNA molecules[34]. The tether length was determined using a calibration curve relating tether length to rho square values (Figure S3). Tethers with anomalous length were excluded.

Magnetic Tweezers (MTs)

Our magnetic tweezers parameters have been previously described [39, 40]. All MTs experiments were conducted at room temperature and a protocol similar to what already described [32] was followed. As shown in Figure S1, the DNA tether, anchored via a stalled RNAP, formed plectonemes under low tension (<1 pN) after the critical torque value was reached. A "hat" curve described the relationship between the extension (ΔZ) of each DNA tether and the number of magnet turns (Figure S4, left) and was used to distinguish whole dsDNA tethers from nicked ones and singly from multiply tethered beads. Before starting a transcription assay, the tethers were first rotated to -19 turns, their extension was then recorded for about 1 minute, after which 1 mM NTPs alone, or with 10 nM LacI, in TXB were introduced to resume transcription.

Estimation of RNAP progress within the loop

When an elongating RNAP is trapped inside a loop, torque will accumulate quickly, the more so, the closer RNAP is to either operator. Since a torque of +11 pN·nm ahead, or -11 pN·nm behind RNAP has been shown to stall its progress [41], the least impediment to RNAP from accumulated torque will occur when the enzyme is in the middle of the loop (half way from the closure) when this forms. At this location, the torque in the flanking DNA can be expressed as:

$$\tau \approx \frac{2\pi k_B T C_{eff}}{L_s} \Delta Lk \quad [42] \qquad (1)$$

Where L_s is the contour length of the flanking DNA, C_{eff} is the effective twist persistence length (twist modulus/k_BT), ΔLk is the linking number change in the DNA. In this study, $L_s \approx$ 200 bp * 3.4/10.5(nm/bp) = 64.8 nm, $C_{eff} \approx$ 63 nm under tension, *f*, in this case is 0.45 pN [43],$k_BT \approx$ 4.1 pN·nm, therefore, the maximum change in linking number that RNAP can induce before stalling ($|\tau| = 11$ pN·nm) is $\Delta Lk = \frac{|\tau| L_s}{2\pi k_B T C_{eff}} = \frac{11*64.8}{2\pi*4.1*80} \approx 0.44$ turns, which corresponds to ΔLk * 10.5 (bp/turn) $\approx$ 5 bp. Thus, 5 bp is the longest that RNAP can transcribe when it happens to be trapped inside a ~400 bp loop and it happens only if the loop closes when RNAP is right in between the two operators.

Estimation of torque at the O1 pause site

Mosconi et al. [43] have shown that under 0.45 pN and 0.8 pN of tension $C_{eff} \approx$ 63 nm and 72 nm, respectively. Thus, designing the experiment such that RNAP reaches O1 after having introduced 5 positive turns into the DNA tether, so that ΔLk = +5, since the length of the DNA tether up to O_1: $L_s \approx$ 3600bp * 3.4/10.5(nm/bp) = 1165 nm, equation (1) yields torque $\tau_{0.45} \approx$ 7.0 pN·nm, $\tau_{0.8} \approx$ 8.0 pN·nm Instead, under 0.25 pN tension RNAP will have introduced a ΔLk = +5 after the buckling transition, where the torque on the DNA stays approximately constant at approximately 4 pN·nm [43].

Results

Elongation through LacI-mediated loops can be monitored by the Tethered Particle Motion Technique (TPM).

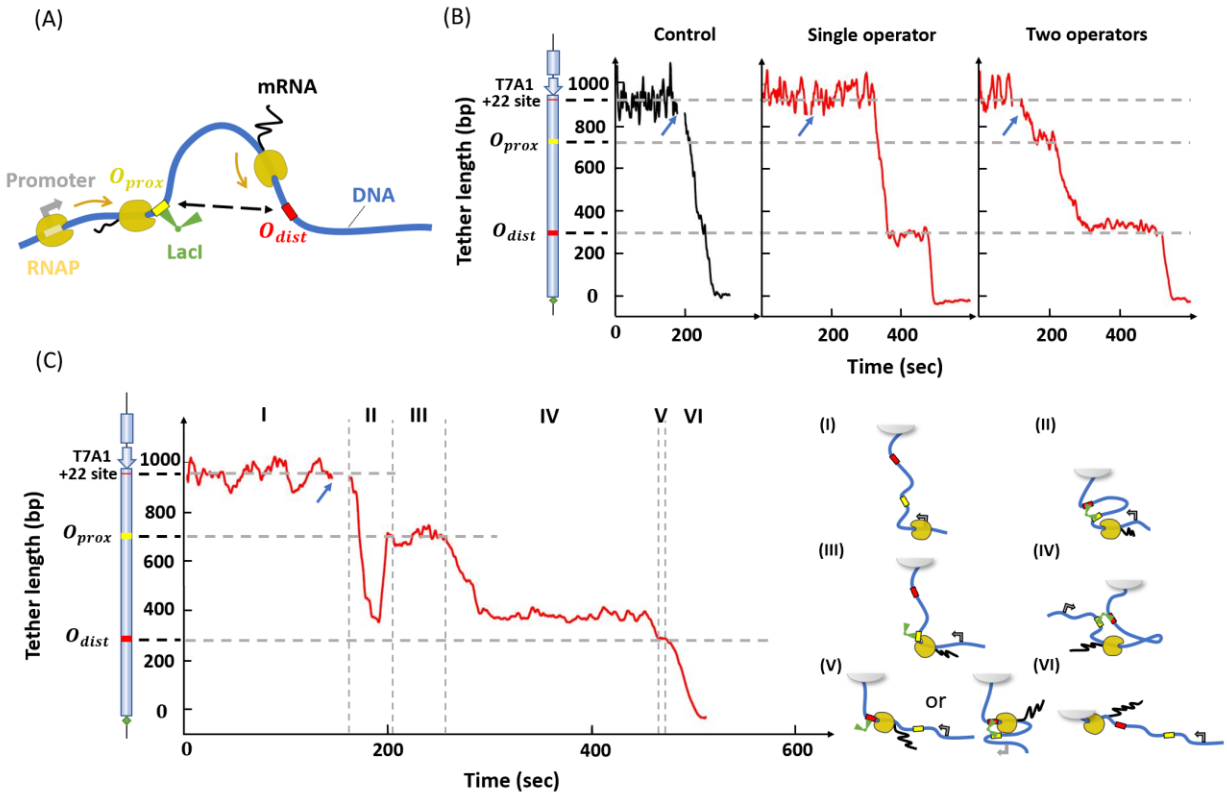

Fig. 1. RNAP can transcribe through a LacI-mediated loop after a pause. (A) The transcription elongation complex is depicted at different stages along the looping template. Curved orange arrows indicate the direction of transcription starting at the promoter. A single LacI may bridge the two operators and induce the formation of a DNA loop. (B) Representative transcription traces. Left: control trace without LacI. Center: transcription in the presence of 10 nM LacI and only the distal operator. Right: transcription in the presence of 10 nM LacI and two operators. At this concentration, each operator is likely to be occupied by a different LacI protein. The blue arrows indicate the time at which NTPs were introduced. (C) Transcription in the presence of 0.2 nM LacI at which looping is likely to occur. The vertical dash lines identify six zones (I - VI) in the progress of RNAP along the DNA template and the cartoons on the right depict the likely conformation of the transcription elongation complex in each zone. The cartoons on the left of the y-axis in panels B and C show the features of the DNA template used in TPM measurements. From top to bottom: a T7A1 promoter, a stall site at +22, a promoter-proximal operator (O_{prox}) and promoter-distal operator (O_{dist}). The dashed horizontal lines indicate the position of the LacI operator(s) in the construct, and the expected location of elongation pauses in the trace.

First, the tethered particle motion (TPM) technique was used to study transcription elongation through the LacI-mediated loop roadblock. As RNAP transcribed through the DNA template containing two binding sites (operators) for the LacI protein (Figure 1A), three scenarios were possible: RNAP could encounter an unencumbered operator, an operator bound by LacI on a linear DNA, or a LacI bridging two operators and securing a DNA loop. Any of these scenarios may change in time: LacI may dissociate from the promoter-proximal operator (O_{prox}), a loop may

(re)form trapping RNAP inside it, and finally, LacI may dissociate from the promoter-distal operator (O_{dist}), letting RNAP proceed to the end of the template. Control experiments with DNA templates containing different combinations of O_{prox} and O_{dist} ((O1, O2), (O2, O1), (Null, O1), (O1, Null)) and appropriate LacI concentrations (Figure S5) were also performed. In all experiments, before addition of the four nucleotides, the TPM signal was constant at a value consistent with the DNA tether length. Addition of NTPs and LacI, indicated by the blue arrow in each of the plots in Figure 1B and C, caused a short-lived disturbance, which was cut out from the recording leaving a short gap in the trace. Then, RNAP resumed elongation as indicated by the smooth decrease in tether length and continued to the end of the template uninterrupted, unless it encountered LacI bound to an operator. Control experiments in the presence of 1 mM NTPs, but in the absence of LacI showed no pausing by RNAP at either of the two operator sites (Figure 1B, left). In the presence of 10 nM LacI, RNAP clearly paused in front of O_{dist} on a DNA tether containing only this operator (O1 operator) (Figure 1B, middle) or paused in front of both O_{prox} and O_{dist} on a DNA tether containing two operators in either combination (O1, O2 or O2, O1) (Figure 1B, right).

The looping probability in a DNA template containing two operators can be adjusted with LacI concentration [26]. For a 400 bp-long loop between the O2 and O1 operators, a maximum looping probability of ~41% could be achieved with 0.2 nM LacI. Increasing LacI concentration to 10 nM increased the probability that each operator is occupied by a different LacI protein, thus only ~6% looping probability could be achieved at this concentration (Figure S5). In the latter conditions, RNAP paused at two positions corresponding to the promoter-proximal and -distal operators, and no looping activity was observed (Figure 1B, right). However, with 0.2 nM LacI, transcription and looping both occurred. Figure 1C shows a representative TPM transcription trace. The trace can be divided into six zones (I-IV) which represent different activities of RNAP along different segments of the template. Zone (I) shows the DNA tether length prior to the addition of 1 mM NTPs and 0.2 nM LacI. Zone (II) starts with the formation of the loop while RNAP was transcribing towards O_{prox} and ends with the loop rupture when RNAP was in front of O_{prox}. Pausing of RNAP at this location suggests that LacI was bound to O_{prox}. In zone (III), RNAP was paused in front of O_{prox} until LacI dissociated from O_{prox}. In zone (IV), RNAP restarted elongation of the inter-operator region from O_{prox} and paused before it reached the distal operator. As long as the loop lasted, RNAP did not elongate, since the length of the tether after the loop ruptured returned to the same height as right before loop formation. However, elongation resumed after loop breakdown and RNAP transcribed to O_{dist}. In zone (V), RNAP paused in front of O_{dist} for a short time, indicating that, upon loop breakdown, LacI remained associated with this operator, then transcribed into zone (VI) after LacI dissociation and, finally, reached the end of the template. Traces, such as this show that transcription through a loop can be followed by TPM.

The strength of the LacI obstacle depends on RNAP position relative to the loop.

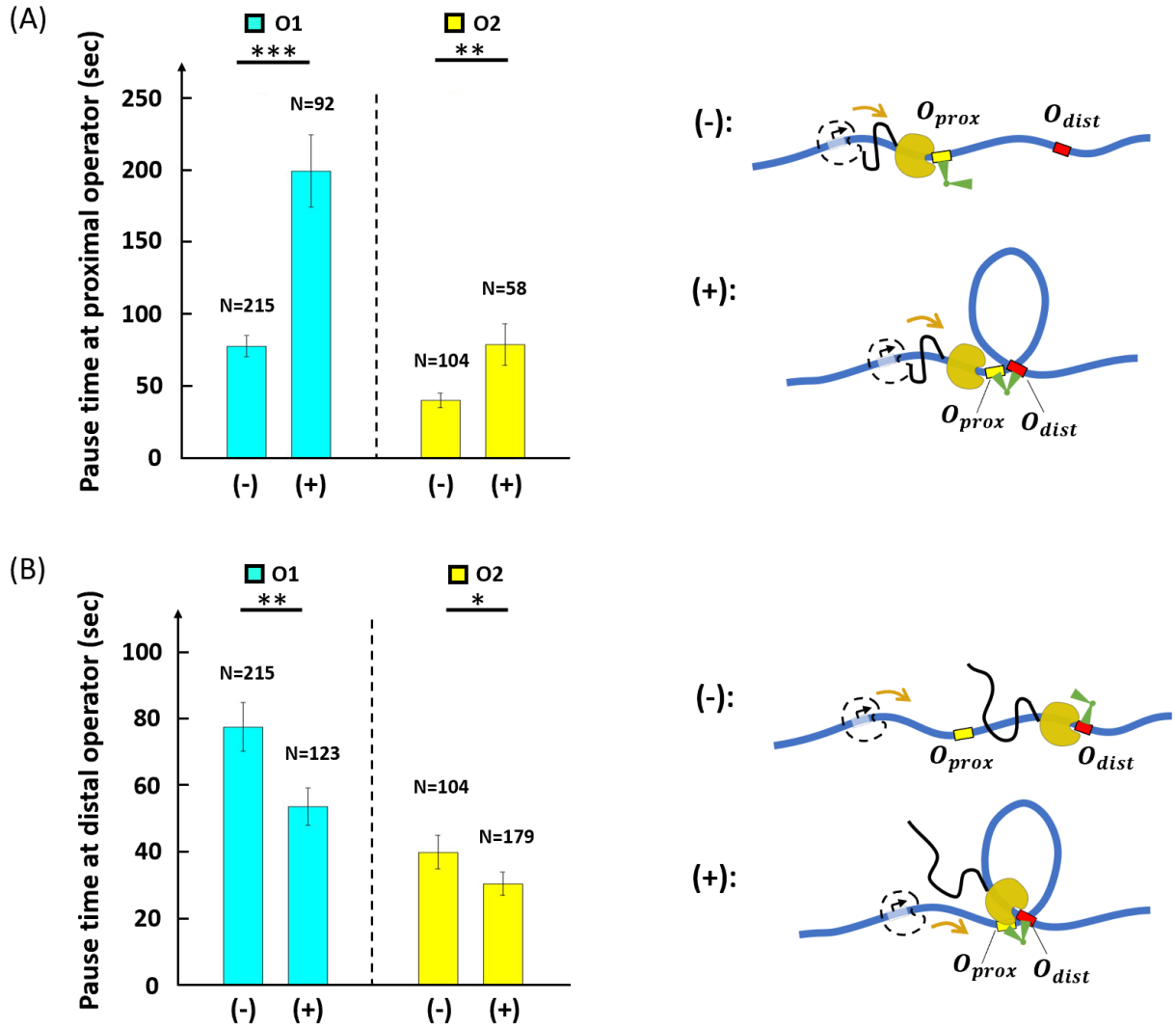

Fig. 2. The LacI-mediated loop has opposite effects on the RNAP pause duration in front of the proximal versus the distal operator. (Left) Average pause duration in front of the (A) proximal operator and (B) distal operator, be it O1 (left, cyan) or O2 (right, yellow), in the absence (-), or presence (+) of a loop. ***$\boldsymbol{p} \leq \mathbf{0.001}$, **$\boldsymbol{p} \leq \mathbf{0.01}$, $*\boldsymbol{p} \leq \mathbf{0.12}$ (two-sample t test). Error bars are standard errors. N values are the number of observations. (Right) Cartoons depicting the two possible types of encounters between RNAP and LacI bound to an operator (O1 or O2) without (-), or with (+), a loop.

Our previous work[32] indiates that when LacI secures a loop, the promoter-proximal, LacI-O2 becomes a stronger obstacle than the linear LacI-O2 complex, thus blocking transcription more effectively. This was observed analyzing static AFM images which, furthermore, captured only a few complexes containing RNAP inside the loop. Thus, to measure the kinetics of RNAP elongation through the loop and understand the effect of looping on the promoter-distal operator-LacI complex, we measured and compared the pause time of RNAP in front of a single operator (Figure 1B, middle) with that of RNAP in front of either O1 or O2 at O_{prox} (Figure 1C, zone III) or O_{dist} (Figure 1C, zone V) in looping conditions. We found that the average pause time of RNAP in front of either the LacI-O1, or LacI-O2, obstacle in the proximal position increased with looping

(Figure 2A, left). RNAP paused in front of the LacI-O1 obstacle for 77 ± 7 s without a loop, but for 199 ± 25 s in the presence of a loop. Similarly, RNAP paused in front of LacI-O2 obstacle increased from 40 ± 5 s without a loop to 79 ± 14 s with a loop. The likely reason for such a prolonged pause is that the effective LacI affinity for the proximal operator increases due to the presence of the distal operator, which increases the local concentration of LacI [26]. The steric hindrance caused by the loop itself may also contribute to the lengthening of the pause before the proximal operator, although this effect is likely to be small [32]. It is also worth noticing that the strength of the LacI-O1 roadblock was increased by looping considerably more (~160%) than the LacI-O2 obstacle (~50%). Likely, this difference is due to the fact that the O1 operator has higher affinity for LacI than the O2 operator, therefore, the loop has a higher probability of forming during RNAP pausing in front of the LacI-O1 than the LacI-O2 obstacle.

Traces such as the ones in the middle and right panels of Figure 1B and in zone (V) of Figure 1C allowed us to compare pause duration at the promoter-distal operator, without or with looping. As RNAP pauses in front of the distal operator, the tether length will not be changed significantly by loop formation because of the experimental setup (Figure S1 A and cartoon (V) on the right of Figure 1C). Therefore, the pause duration measured in front of O_{dist} will be a mix of pauses in front of LacI engaged, or not, in loop closure with 41% probability of it securing a loop, given the 0.2 nM LacI concentration used (Figure S5). Comparison of pause times (Figure 2B, left histogram) with and without looping shows, surprisingly, that the average pause time of RNAP in front of the distal LacI-O1, or -O2, obstacle is shortened to 54 ± 6 s and 30 ± 4 s , respectively, relative to pausing observed under conditions without possible looping, 77 ± 7 and 40 ± 5 s, respectively. The difference becomes even larger after accounting for the 60% contribution of the pauses in front of a LacI not securing a loop (Figure 1B). Indeed, inside the loop, RNAP pauses just for approximately (54 - 0.6*77) / 0.4 ≈ 20 s at the distal O1 operator, and for (30 - 0.6*40) / 0.4 ≈ 15 s at the distal O2 operator. These results suggest that the loop significantly weakens the roadblocking effect of the LacI-distal operator obstacle. Clearly, the increased local concentration, due to cooperativity between the two operators, must not play a dominant role in determining the effect of looping on pausing at the distal operator, regardless of the affinity of the operator.

The LacI-mediated loop can trap RNA polymerase.

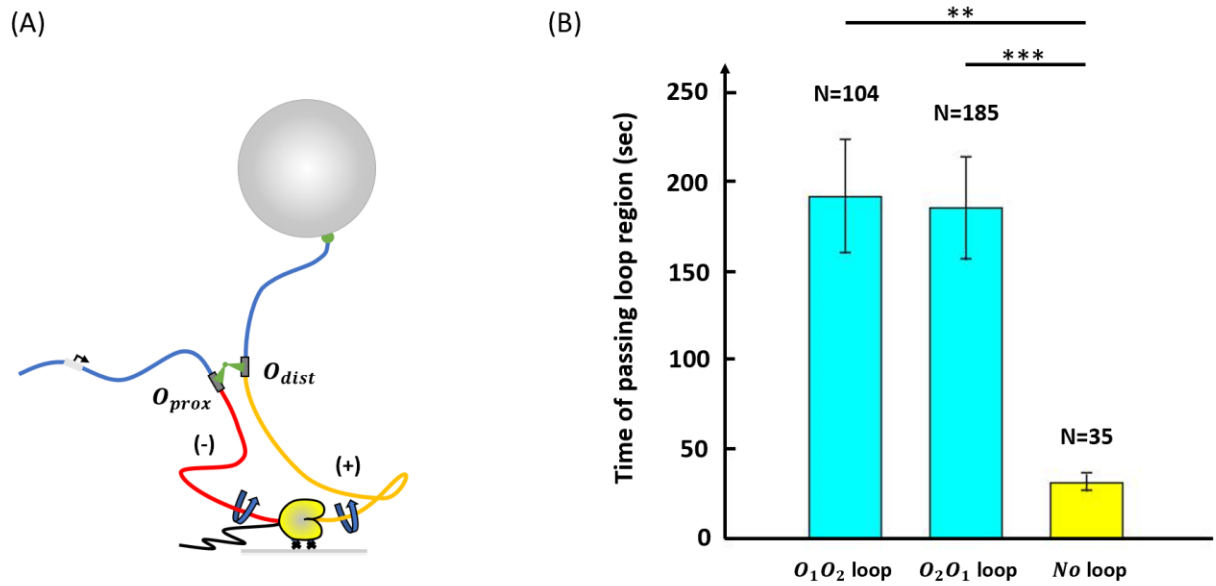

Fig. 3. Loop delays RNAP progress. (A) A cartoon depicting RNAP trapped inside the loop. A bent black arrow indicates the promoter, blue DNA is torsionally relaxed, red DNA is unwound, yellow DNA is overwound, nascent RNA is the black curvy line exiting from RNAP. (B) Time needed for RNAP to transcribe past the loop region with (cyan bars) or without (yellow bar) looping. ***$p \leq 0.001$, **$p \leq 0.01$ (two-sample t test). Error bars are standard error. N values are the sample sizes.

Segment IV in Figure 1C shows that a protein-mediated loop can significantly delay RNAP progression. According to the twin-supercoiled-domain model [27], an elongating RNAP untwists DNA upstream, generating negative supercoiling (Figure 3A, red DNA) and twists DNA downstream, generating positive supercoiling (Figure 3A, yellow DNA). Furthermore, LacI can divide a supercoiled DNA molecule into two independent topological domains [44]. Thus, the LacI-mediated loop is a topologically isolated domain that can constrain the torsional stress generated by an elongating RNAP. If a loop encircles an elongating RNAP, torsional stress in the 400 bp-long loop can accumulate to +11 pN·nm ahead of RNAP or -11 pN·nm behind in a short time, stalling RNAP [41]. Upon stalling, RNAPs are prone to backtracking, and the recovery from the backtracked state is slow. RNAP can only advance up to approximately five nucleotides after the 400 bp loop forms around it (Materials and Methods). Thus, we measured the total time spent by RNAP transcribing the entire loop region (duration of zone IV in Figure 1C) and compared it with the time required to elongate between the two operators in the absence of LacI/looping (Figure 1B, left control trace). The average transcription time of the O_1O_2 and O_2O_1 loops was 192 ± 31 s and 185 ± 29 s, respectively. Both these times were much longer than the average time without looping (32 ± 5 s). We conclude that the LacI loop can significantly delay RNAP progress by encircling it.

Positive supercoiling inside the loop helps RNAP escape

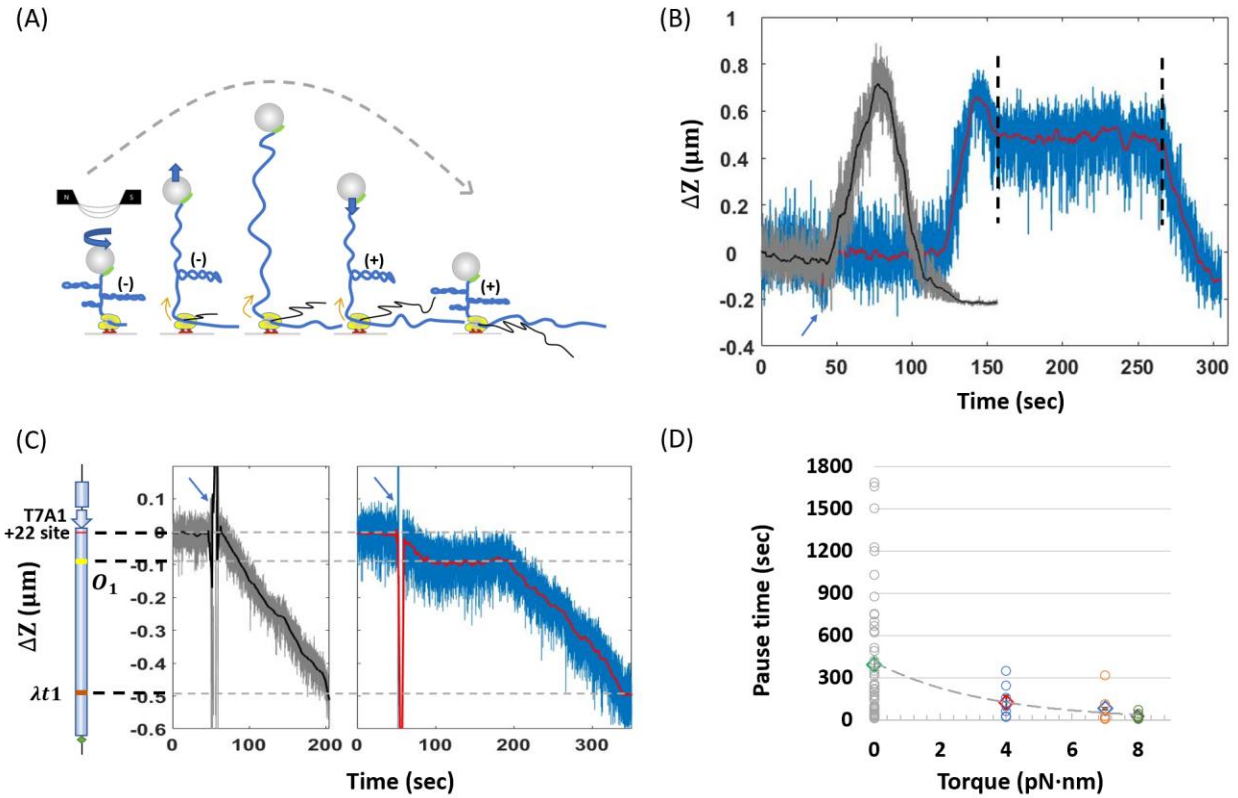

Fig. 4. Comparison of RNAP pause times at O1 with and without positive supercoiling. (A) Description of the experimental strategy and expected tether length change during transcription. The dashed gray arrow indicates the progressive conversion of negative to positive plectonemes due to RNAP transcriptional activity. (B) Overlay of representative RNAP transcription traces without (gray) and with (blue and red) LacI on a template pre-loaded with negative supercoiling. The blue arrow indicates the time at which NTPs, or NTPs+LacI were introduced. The two vertical black dashed lines mark the duration of the RNAP pause in front of the LacI-O1 operator complex. (C) DNA diagram and representative elongation traces in the absence of pre-loaded supercoiling without (left panel, gray and black), and with (right panel, blue and red) LacI. (D) Pause times in front of O1 under different torsional stress. Torque values were calculated using Eq 1 in reference 38, with caveat that C_{eff} was estimated in 100 mM [Na+] instead of 50 mM [K+]. Circles represent individual pause times, diamonds represent average pause times.

The data in Figure 2 showed that the loop weakens the blocking effect of the distal LacI-operator obstacle. We hypothesized that the shorter pause time in front of the distal operator is due to the fact that LacI is destabilized by the positive supercoiling generated by RNAP inside the loop, since this can encircle the enzyme and act as a barrier to supercoiling diffusion. In our TPM experimental setup, the DNA segments flanking the loop (blue DNA segment in Figure 3 A) can quickly release any torsional stress due to RNAP transcriptional activity because the upstream DNA is free, and the downstream DNA is attached to the bead through a single bond (Figure S1A). Within the loop, however, positive supercoiling ahead of RNAP accumulates and might cause LacI to dissociate from the distal operator. To test this hypothesis, we used magnetic tweezers (MTs) to follow elongation of an RNAP transcribing toward a LacI-O1 obstacle on a construct where the downstream DNA could be positively supercoiled (Figure 4A, Figure S1B). In the experimental setup we designed, the region between RNAP and the tethered bead is torsionally

constrained by a tail of biotin-streptavidin linkages under a range of forces between approximately 0.25 and 0.8 pN. The DNA template was preloaded with negative plectonemes (Figure 4A) to make sure that RNAP did not stall due to excessive positive supercoiling before it reached the obstacle. As transcription progressed, the expected DNA tether length changed as depicted in Figure 4A. In the template we built, RNAP needed to transcribe for 252 base pairs (approximately 24 turns) before reaching the O1 operator (Figure S1B). Thus, we first verified that RNAP could transcribe a tether preloaded with -24 turns (gray and black trace in Figure 4B). After introducing NTPs (blue arrow in Figure 4B), the tether extension increased, due to annihilation of the negative supercoiling by the positive supercoiling generated by the elongating RNAP, until the DNA tether became torsionally relaxed. After that, RNAP continued to wind the DNA tether introducing positive plectonemes until the tether was so short that the bead reached the surface of the flow-chamber, or RNAP was not able to progress further due to either steric hindrance by the plectonemes, or large torsional stress. Once the ability of RNAP to transcribe a template negatively supercoiled by several turns was assessed, we designed a transcription measurement in the presence of LacI in which RNAP reached the O1 operator after having introduced in the DNA template a ΔLk = +5 because, according to the "hat" curve (Figure S4B, left), the tether length with +5 turns can be clearly distinguished from a relaxed tether (ΔLk = 0). Therefore, since RNAP positively twists DNA for 24 turns before it encounters the O1 operator, we chose to pre-load the template with -19 turns before restarting transcription from the stall site. The blue and red traces in Figure 4B are the raw data and 4s average, respectively, of a measurement with 10 nM LacI. Although RNAP paused also at random positions along the trace, the expected pause at O1 was clearly distinguishable (Figure 4B, between vertical, black, dashed lines, see Figure S4 for identification of the O1 position). For comparison, we acquired MT measurements of the RNAP pause in front of the LacI-O1 obstacle on torsionally relaxed DNA under 0.45 pN tension (Figure 4C right, Figure S1B). Figure 4D shows how pause time changes with different torque applied on DNA. The average pause time of RNAP at the LacI-O1 obstacle with no torque τ_1 = 0 pN·nm gray circles, green diamond) was 393 ± 64 s which is much longer than the average pause time with positive torque τ_2 ≈ 4 pN·nm (blue circles & red diamond), τ_3 ≈ 7 pN·nm (orange circles & blue diamond for torque) and τ_4 ≈ 7 pN·nm (green circles & purple diamond), which pause RNAP for 125 ± 42 s, 82 ± 50 s and 26 ± 8 s, respectively. This result indicates that positive supercoiling can significantly facilitate RNAP passing the Lac-O1 obstacle and, likely, the LacI-O2 obstacle as well. The decrease in pause duration as positive torque on DNA increased suggests that positive supercoiling weakens LacI binding, thereby relieving its roadblock effect. Positive supercoiling generated by RNAP translocation is also known to destabilize nucleosomes [31, 45]; it may, therefore, represent a general mechanism by which RNAP may transcribe through protein roadblocks along the DNA.

Discussion

Our results reveal a dynamic interplay between the LacI-stabilized DNA loop and transcription of the looped DNA segment. While the roadblock strength on the linear DNA is determined by the LacI affinity for the operator DNA, our TPM measurements show that looping can alter the roadblock effect of LacI-operator obstacles in opposite ways depending on the position of the roadblock relative to the promoter: the strength of the proximal roadblock increases upon formation of the loop, whereas that of the distal roadblock is weakened. An increase in pause duration of the RNAP approaching the loop is likely due to the fact that the loop effectively increases the LacI concentration in the vicinity of the operator [26], therefore decreasing the probability of dissociation, and increases the steric hindrance that the loop represents for an

approaching RNAP [32]. Once RNAP enters the loop, it is significantly slowed down, taking six time longer to traverse this region relative to transcription on the unlooped DNA. However, once the RNAP approaches the distal operator, it can dislodge the roadblock more readily, as reflected by the shorter pause duration in front of the distal LacI-operator.

To explain the shorter pause in front of the LacI-distal operator securing a loop, we found, using MTs, that positive supercoiling between the enzyme and the roadblock shortens the pause of RNAP in front of the protein. This result supports our hypothesis that positive supercoiling generated by RNAP transcriptional elongation inside the loop helps RNAP exiting the loop, likely dislodging the LacI obstacle from the distal operator. In general, accumulated positive supercoiling ahead of RNAP may accelerate protein dissociation from DNA and reduce the pause time in front of a protein-mediated loop.

We conclude that small loops of few hundred base pairs, such as the one investigated here and those induced by many prokaryotic regulators, seem to effectively trap RNAP, and to eventually release it when the positive torsional stress exceeds a critical threshold. Additional experiments to support this hypothesis, using topoisomerase IB, or a nicking enzyme targeted to the loop region, were not feasible. The delay in topoisomerase IB activity prevented us from carrying out the experiment. Nicking of either DNA strand, instead, induces RNAP pausing, or fortuitous transcription initiation, at the nicking site.

In *vivo*, the ability of protein-mediated loops to trap RNAP may be a critical factor in the regulation of transcription at the local level. In the eukaryotic organism *Drosophila melanogaster*, it was observed, using 4C-seq assays, that RNA polymerase II was often paused near promoters involved in long-range interactions via several kilobase pair-long loops with enhancers. The hypothesis proposed was that since paused promoters can exert enhancer-blocking activity[46], the presence of paused polymerase could safeguard against premature transcriptional activation, but yet keep the system poised for activation.[47] It is possible that RNAP pausing during elongation, either in front, or within, a regulatory loop formed in an actively transcribed region is part of a mechanism to (i) wait for additional factors to resolve the loop or relieve supercoiling as a signal to resume transcription, or (ii) downregulate transcription of a gene. We propose that while transient stalling inside a loop may be important to enable RNAP to respond to regulatory inputs, RNAP has an intrinsic ability to elongate through protein-DNA roadblocks. As long as it is able to recover from a stall, sometimes aided by accessory proteins, RNAP can actively dislodge roadblock thanks to the positive supercoiling it generates ahead. Given the ubiquity of looping in any genome, mechanisms that enable RNAP transcription through loops must also be ubiquitous, controlling the chromosome compaction and gene expression.

Acknowledgments

LacI was a generous gift from Kathleen Matthews.

This work was supported by the National Institutes of Health (NIH) R01 grants GM084070 (L.F.) and GM067153 (I.A.).

References

[1] Ahmed, S. M., and Droge, P. (2020) Chromatin Architectural Factors as Safeguards against Excessive Supercoiling during DNA Replication, *International Journal of Molecular Sciences 21*.

[2] Kantidze, O. L., and Razin, S. V. (2020) Weak interactions in higher-order chromatin organization, *Nucleic Acids Research 48*, 4614-4626.
[3] Krogh, T. J., Franke, A., Moller-Jensen, J., and Kaleta, C. (2020) Elucidating the Influence of Chromosomal Architecture on Transcriptional Regulation in Prokaryotes - Observing Strong Local Effects of Nucleoid Structure on Gene Regulation, *Frontiers in Microbiology 11*.
[4] Arnould, C., and Legube, G. (2020) The Secret Life of Chromosome Loops upon DNA Double-Strand Break, *Journal of Molecular Biology 432*, 724-736.
[5] Banigan, E. J., and Mirny, L. A. (2020) Loop extrusion: theory meets single-molecule experiments, *Current Opinion in Cell Biology 64*, 124-138.
[6] Cacciatore, A. S., and Rowland, B. D. (2019) Loop formation by SMC complexes: turning heads, bending elbows, and fixed anchors, *Current Opinion in Genetics & Development 55*, 11-18.
[7] Gramzow, L., Ritz, M. S., and Theissen, G. (2010) On the origin of MADS-domain transcription factors, *Trends in Genetics 26*, 149-153.
[8] Hansen, A. S., Cattoglio, C., Darzacq, X., and Tjian, R. (2018) Recent evidence that TADs and chromatin loops are dynamic structures, *Nucleus (Austin, Tex.) 9*, 20-32.
[9] Hosokawa, H., and Rothenberg, E. V. How transcription factors drive choice of the T cell fate, *Nature Reviews Immunology*.
[10] Lazniewski, M., Dawson, W. K., Rusek, A. M., and Plewczynski, D. (2019) One protein to rule them all: The role of CCCTC-binding factor in shaping human genome in health and disease, *Seminars in Cell & Developmental Biology 90*, 114-127.
[11] Umlauf, D., and Mourad, R. (2019) The 3D genome: From fundamental principles to disease and cancer, *Seminars in Cell & Developmental Biology 90*, 128-137.
[12] Pavco, P. A., and Steege, D. (1990) Elongation by Escherichia coli RNA polymerase is blocked in vitro by a site-specific DNA binding protein, *Journal of Biological Chemistry 265*, 9960-9969.
[13] Petesch, S. J., and Lis, J. T. (2012) Overcoming the nucleosome barrier during transcript elongation, *Trends Genet 28*, 285-294.
[14] Kulaeva, O. I., Hsieh, F.-K., Chang, H.-W., Luse, D. S., and Studitsky, V. M. (2013) Mechanism of transcription through a nucleosome by RNA polymerase II, *Biochimica et Biophysica Acta (BBA)-Gene Regulatory Mechanisms 1829*, 76-83.
[15] Sanders, T. J., Lammers, M., Marshall, C. J., Walker, J. E., Lynch, E. R., and Santangelo, T. J. (2019) TFS and Spt4/5 accelerate transcription through archaeal histone-based chromatin, *Mol Microbiol 111*, 784-797.
[16] Dodd, I. B., and Egan, J. B. (2002) Action at a distance in Cl repressor regulation of the bacteriophage 186 genetic switch, *Molecular Microbiology 45*, 697-710.
[17] Gramzow, L., and Theissen, G. (2010) A hitchhiker's guide to the MADS world of plants, *Genome Biology 11*.
[18] Guerra, R. F., Imperadori, L., Mantovani, R., Dunlap, D. D., and Finzi, L. (2007) DNA compaction by the nuclear factor-Y, *Biophysical Journal 93*, 176-182.
[19] Lee, B. K., and Iyer, V. R. (2012) Genome-wide Studies of CCCTC-binding Factor (CTCF) and Cohesin Provide Insight into Chromatin Structure and Regulation, *Journal Of Biological Chemistry 287*, 30906-30913.
[20] Mack, C. P., Thompson, M. M., Lawrenz-Smith, S., and Owens, G. K. (2000) Smooth muscle alpha-actin CArG elements coordinate formation of a smooth muscle cell-selective, serum response factor-containing activation complex, *Circulation Research 86*, 221-232.
[21] Mendes, M. A., Guerra, R. F., Berns, M. C., Manzo, C., Masiero, S., Finzi, L., Kater, M. M., and Colombo, L. (2013) MADS Domain Transcription Factors Mediate Short-Range DNA Looping That Is Essential for Target Gene Expression in Arabidopsis, *Plant Cell 25*, 2560-2572.
[22] Miano, J. M. (2008) Deck of CArGs, *Circulation Research 103*, 13-15.

[23] Miwa, T., Boxer, L. M., and Kedes, L. (1987) CARG Boxes in the Human Cardiac Alpha-Actin Gene Are Core Binding Sites for Positive Trans-Acting Regulatory Factors *Proceedings Of The National Academy Of Sciences Of The United States Of America 84*, 6702-6706.
[24] Vörös, Z., Yan, Y., Kovari, D. T., Finzi, L., and Dunlap, D. (2017) Proteins mediating DNA loops effectively block transcription, *Protein Science 26*, 1427-1438.
[25] Becker, N. A., Peters, J. P., Maher, L. J., 3rd, and Lionberger, T. A. (2013) Mechanism of promoter repression by Lac repressor-DNA loops, *Nucleic Acids Res 41*, 156-166.
[26] Priest, D. G., Cui, L., Kumar, S., Dunlap, D. D., Dodd, I. B., and Shearwin, K. E. (2014) Quantitation of the DNA tethering effect in long-range DNA looping in vivo and in vitro using the Lac and lambda repressors, *Proc Natl Acad Sci U S A 111*, 349-354.
[27] Liu, L. F., and Wang, J. C. (1987) Supercoiling of the DNA template during transcription, *Proc Natl Acad Sci U S A 84*, 7024-7027.
[28] Yan, Y., Ding, Y., Leng, F., Dunlap, D., and Finzi, L. (2018) Protein-mediated loops in supercoiled DNA create large topological domains, *Nucleic Acids Res 46*, 4417-4424.
[29] Whitson, P. A., Hsieh, W. T., Wells, R. D., and Matthews, K. S. (1987) Supercoiling Facilitates Lac Operator-Repressor-Pseudooperator Interactions, *Journal of Biological Chemistry 262*, 4943-4946.
[30] Barkley, M. D., Barkley, M. D., and Bourgeoi.S. (1974) MEASUREMENTS OF UNWINDING OF LAC OPERATOR BY REPRESSOR, *Nature 251*, 247-249.
[31] Sheinin, M. Y., Li, M., Soltani, M., Luger, K., and Wang, M. D. (2013) Torque modulates nucleosome stability and facilitates H2A/H2B dimer loss, *Nat Commun 4*, 2579.
[32] Voros, Z., Yan, Y., Kovari, D. T., Finzi, L., and Dunlap, D. (2017) Proteins mediating DNA loops effectively block transcription, *Protein Sci 26*, 1427-1438.
[33] Svetlov, V., and Artsimovitch, I. (2015) Purification of bacterial RNA polymerase: tools and protocols, *Methods Mol Biol 1276*, 13-29.
[34] Kumar, S., Manzo, C., Zurla, C., Ucuncuoglu, S., Finzi, L., and Dunlap, D. (2014) Enhanced tethered-particle motion analysis reveals viscous effects, *Biophys J 106*, 399-409.
[35] Han, L., Lui, B. H., Blumberg, S., Beausang, J. F., Nelson, P. C., and Phillips, R. (2009) Calibration of tethered particle motion experiments, In *Mathematics of DNA structure, function and interactions*, pp 123-138, Springer.
[36] Ucuncuoglu, S., Schneider, D. A., Weeks, E. R., Dunlap, D., and Finzi, L. (2017) Multiplexed, tethered particle microscopy for studies of DNA-enzyme dynamics, In *Methods in enzymology*, pp 415-435, Elsevier.
[37] Kovari, D. T., Yan, Y., Finzi, L., and Dunlap, D. (2018) Tethered Particle Motion: An Easy Technique for Probing DNA Topology and Interactions with Transcription Factors, *Methods Mol Biol 1665*, 317-340.
[38] Priest, D. G., Kumar, S., Yan, Y., Dunlap, D. D., Dodd, I. B., and Shearwin, K. E. (2014) Quantitation of interactions between two DNA loops demonstrates loop domain insulation in E. coli cells, *Proceedings of the National Academy of Sciences 111*, E4449-E4457.
[39] Finzi, L., and Dunlap, D. D. (2010) Single-molecule approaches to structure, kinetics and thermodynamics of transcriptional regulatory nucleoprotein complexes", *J. Biol. Chem. 285*, 18973-18978.
[40] Kovari, D. T., Dunlap, D., Weeks, E. R., and Finzi, L. (2019) Model-free 3D localization with precision estimates for brightfield-imaged particles, *Opt. Express 27*, 29875-29895.
[41] Ma, J., Bai, L., and Wang, M. D. (2013) Transcription under torsion, *Science 340*, 1580-1583.
[42] Moroz, J. D., and Nelson, P. (1997) Torsional directed walks, entropic elasticity, and DNA twist stiffness, *Proc Natl Acad Sci U S A 94*, 14418-14422.

[43] Mosconi, F., Allemand, J. F., Bensimon, D., and Croquette, V. (2009) Measurement of the torque on a single stretched and twisted DNA using magnetic tweezers, *Phys Rev Lett 102*, 078301.
[44] Leng, F., Chen, B., and Dunlap, D. D. (2011) Dividing a supercoiled DNA molecule into two independent topological domains, *Proceedings of the National Academy of Sciences 108*, 19973-19978.
[45] Teves, S. S., and Henikoff, S. (2014) Transcription-generated torsional stress destabilizes nucleosomes, *Nat Struct Mol Biol 21*, 88-94.
[46] Chopra, V. S., Cande, J., Hong, J. W., and Levine, M. (2009) Stalled Hox promoters as chromosomal boundaries, *Genes & Development 23*, 1505-1509.
[47] Ghavi-Helm, Y., Klein, F. A., Pakozdi, T., Ciglar, L., Noordermeer, D., Huber, W., and Furlong, E. E. M. (2014) Enhancer loops appear stable during development and are associated with paused polymerase, *Nature 512*, 96-+.